*Q. J. R. Meteorol. Soc.* (1990), **116**, pp. 363–378 551.554:551.558.21(941)

# Airflow over a two-dimensional escarpment. II: Hydrostatic flow

By R. O. PITTS and T. J. LYONS[1]

*Environmental Science, School of Biological and Environmental Sciences, Murdoch University, Australia*

(Received 25 March 1989; revised 17 July 1989)

SUMMARY

Hydrostatically dominated forced flow over the asymmetric topography of the Darling Scarp, Western Australia, is modelled using a hydrostatic numerical mesoscale model and compared with observations. Simulations reproduce the essential features of wave overturning and the development of a shooting hydraulic flow. This response is dependent on the wind profile but not on the existence of a critical level. The high backsheared environment leads to a high ratio of the Brunt–Väisälä frequency to wind speed throughout the profile, resulting in short wavelengths, high nonlinearity and overturning. With the ratio of the halfwidth of the topography to the boundary-layer depth being small, the flow fields are shown to be sensitive to the boundary layer.

## 1. INTRODUCTION

Forced flows have been extensively modelled using both analytical and numerical techniques, although most analytical studies have been limited to bell-shaped hills. Smith (1979) defined topographically forced waves in terms of the mountain wavenumber, $k$, and the Scorer parameter, $l$, given by

$$l^2 = N^2/U^2 - U^{-1}(d^2U/dz^2)$$

where $U$ is the wind speed and $N$ the Brunt–Väisälä frequency. In particular, assuming that $l$ is independent of height, $l^2 < k^2$ results in evanescent waves that are exponentially damped in the vertical, whereas with $l^2 > k^2$, strong buoyancy effects produce freely propagating waves (Smith 1979). A vertically propagating wave produced by a symmetric mountain with a constant-$U$ and -$N$ atmosphere will overturn for an inverse Froude number ($Nh/U$, where $h$ is the mountain height) of 0·85 and at 0·75 of the vertical wavelength, whereas for asymmetric topography, with gentle windward and steep leeward slopes, overturning occurs at a lower inverse Froude number and at 0·5 the vertical wavelength (Lilly and Klemp 1979).

When $l$ decreases with height, such that $l^2 > k^2$ in the lower levels and $l^2 < k^2$ aloft, a trapped lee wave or resonance wave may be produced (Smith 1979). Physically, this implies a strongly stable layer in the lower atmosphere and/or strongly increasing wind speed with height.

Highly nonlinear flows occur where the perturbations from the initial state are no longer small. These flows are associated with strong downslope winds and in cases where the wave overturns, severe turbulence, as well as the extraction of momentum from the atmosphere in that region. The rapid increase in wave drag and movement of the position of maximum surface wind further down the slope, as observed by Lilly and Zipser (1972), have been explained in terms of the linear reflection mechanism of Klemp and Lilly (1975), the critical-level reflection theory of Peltier and Clark (1979) and as an analogy to the hydraulic jump initially proposed by Long (1954).

The linear reflection theory of Klemp and Lilly (1975) assumes that the final nonlinear state can be reached through the linear partial reflection of waves. Since this is based on linear theory, its applicability to large amplitude waves is yet to be firmly demonstrated (Durran 1986).

[1] Currently on leave from Murdoch University at Department of Meteorology and Wind Energy, Riso National Laboratory, Denmark.

Clark and Peltier (1977, 1984) and Peltier and Clark (1979, 1983) assumed that a critical level (where the wind velocity drops to zero) acts as a linear reflector to the wave energy when the Richardson number is below 0·25 and the height of the critical level is such that the reflected waves are in phase with the incident waves. Peltier and Clark (1979) found that for the highly nonlinear case in which wave breaking occurs (i.e. overturning and convective breakdown) a new regime results in the flow where the wave drag increases substantially above that of the nonbreaking wave. They ascribed this increase to the symmetric mountain producing overturning and hence a critical level at precisely the right height at which the cavity would be tuned. Hence for symmetric mountains, overturning produces a self-induced tuned critical level and amplification. Clark and Peltier (1984) performed simulations for an environmental critical layer and found that the high drag states occurred when the environmental critical layer was at 0·75, 1·75 and 2·75 of the wavelength respectively.

Windstorms have been described in terms of hydraulic flows by Long (1954) and, more recently, by Smith (1985), Durran (1986), Smith and Sun (1987), Durran and Klemp (1987) and Bacmeister and Pierrehumbert (1988). Smith (1985), using observational data (Lilly 1978) and results from the numerical modelling of Peltier and Clark (1979), derived an idealized picture of the severe wind configuration. This consisted of a region of stagnant, turbulent adiabatic air developing in the middle to upper troposphere underneath which developed a laminar flow which descended and accelerated over the mountain and down its lee slope. Assuming also that there is a dividing streamline underneath which the shooting flow accelerates, he derived an analytical model which was able to predict the altitude of turbulent air, the strength of winds and mountain drag.

Smith's model predicted that for an effective mountain height ($Nh/U$) there would be only one height of the initial dividing streamline which would lead to this flow. Durran (1986) showed that the rapid amplification of the wave after overturning, as first observed by Peltier and Clark (1979), could be described as a transition from a vertically propagating wave to a hydraulic jump with the development of a shooting flow down the lee slope. This occurred in his two-layer solutions when the pressure gradient caused by the interface displacement dominated the other contributions to the total pressure perturbations along the lee slope.

Durran and Klemp (1987), using a preset environmental critical level similar to that of Clark and Peltier (1984), but a larger range of parameters, were able to show that this transition to a high drag state occurred at the heights predicted by Smith's (1985) theory and not by that of Clark and Peltier. Bacmeister and Pierrehumbert (1988) supported this and also showed that a hydraulic flow could develop when the initial critical level is below the lowest predicted resonant height as found in Durran and Klemp (1987). In this case an upstream propagating bore is generated which adjusts conditions to allow a high drag state (Bacmeister and Pierrehumbert 1988).

Under strong synoptic easterlies, Pitts and Lyons (1989) observed forced flow over the highly asymmetric topography of the 300 m-high north/south oriented Darling Scarp, Western Australia. These observations were characterized by shallow surface gradient winds of 10–20 $m\,s^{-1}$ with an inherent critical level aloft and a stable layer produced through nocturnal radiational cooling. Pitts and Lyons suggested that the flows could be differentiated by an average hydrostatic index, $Na/U$, where $a$ is the mountain halfwidth, with index values above 4·8 leading to hydrostatically dominated flow.

For two such hydrostatically dominated days, they suggested that the resulting flows were formed through two distinct mechanisms. In one case, a vertically propagating hydrostatic wave appeared to form through resonant amplification, in accord with the theory of Clark and Peltier (1984). The other flow represented a direct analogy to classical

two-layered hydraulic flow. In this instance, the existence of a sharp inversion and a near-neutral layer aloft restricted the vertical propagation of wave energy, resulting in a hydraulic jump (Pitts and Lyons 1989).

Thus this paper presents simulations of these two days based on a hydrostatic numerical mesoscale model, to investigate the processes leading to their formation as well as the sensitivity of the response to the flow parameters.

## 2. Model

Following Mahrer and Pielke (1978) and Hoinka (1985), the numerical meteorological model, originally developed by Pielke (1974) and adapted by McNider and Pielke (1981), was used to simulate the forced flows over the Darling Scarp. Pielke and Mahrer (1975) and Mahrer and Pielke (1977) used an earlier version of the model in their simulations, incorporating an upstream differencing scheme to approximate the advective terms and without an absorbing layer below the top of the model. These were criticized by Klemp and Lilly (1978) on the basis that the upstream differencing substantially overdamped the solutions and was similar in effect to bringing a damping layer down to the surface. Mahrer and Pielke (1978) improved the model by approximating the advective terms by upstream interpolation with a cubic spline and using an absorbing layer as recommended by Klemp and Lilly. They validated the model against an analytical solution of airflow over a 10 m bell-shaped hill as well as by comparison with Klemp and Lilly's (1978) simulation of flow over a 1 km bell-shaped mountain.

Hoinka (1985) provided a more systematic verification of the model against analytical models of both linear and nonlinear flows as well as observational data. His simulations included replacing the constant horizontal exchange coefficients used by Mahrer and Pielke (1978), implementing the absorbing layer formulation of Durran and Klemp (1983) and incorporating the boundary conditions of Klemp and Lilly (1978). The success of these simulations in successfully reproducing both analytic results as well as observational data, highlights the versatility of the model in simulating forced flows as well as its proven ability to simulate thermally driven flows such as sea breezes (Pielke 1974; Pielke and Mahrer 1978).

The model we have used is essentially identical to that described by McNider and Pielke (1981). However, the horizontal diffusion term has been replaced by an implicit filter after Long (McNider and Pielke 1984) given by

$$(1-\beta)\phi_{i+1}^{t+1} + 2(1+\beta)\phi_i^{t+1} + (1-\beta)\phi_{i-1}^{t+1} = \phi_{i+1}^{t} + 2\phi_i^{t} + \phi_{i-1}^{t}$$

where $\phi_i^{t+1}$ is the filtered value at grid point $i$, $\phi_i^t$ is the original value and $\beta$ is the filter coefficient. Using a value of 0·05 for the filter coefficient selectively damps small wavelength features, removing all $2dx$ waves, where $dx$ is the horizontal grid spacing, but $4dx$ waves and larger would retain better than 95% of their original amplitude (Mahrer and Pielke 1978).

In the upper levels of the model, an absorbing layer has been employed using Rayleigh damping, similar to that used by Durran and Klemp (1983) and Hoinka (1985). This has been applied by adding a damping term, $R_u$, to the flow and potential temperature equations, where $R_u = r(z)(u - \bar{u})$. The damping coefficient, $r(z)$, follows a sinusoidal form in the absorbing layer with the value of the coefficient (Table 1) chosen so that the dominant horizontal wavelengths are absorbed most efficiently (Durran and Klemp 1983).

Within the model, the vertical diffusion coefficient is defined by a local or nonlocal scheme depending on the stability (McNider and Pielke 1981). However, in all of our

TABLE 1. MODEL DEFINITION

Model dimensions
Horizontal 100 Grid length 0·5333 km
Vertical 42 (46)
Vertical grid levels 10, 30, 65, 110, 170, 230, 290, 350, 410, 470, 530, 590, 650, 710, 770, 830, 890, 950, 1020, 1120, 1220, 1320, 1420, 1520, 1620, 1720, 1820, 1920, 2020, 2120, 2220, 2370, 2600, 2900, 3300, 3800, 4400, 5000, 5600, 6200, 6800, 7400 m (8400, 9400, 10400, 11400 m)

Surface roughness length ($z_o$) 50 cm

Time step 5·0 s

Long filter coefficient ($\beta$) 0·05

Absorbing layer

Height 35 3300 m
(39) 5600 m

Absorption coefficient 0·01

With no critical level present, four additional layers were used to model wave propagation vertically and these are shown in brackets.

simulations, the boundary layer is prescribed as stable and has no surface heating. Thus only the local scheme, involving mixing length and a critical Richardson number (Blackadar 1979), is used. Consequently, unlike other workers simulating flow over two-dimensional features, we have retained the north/south component of the flow when the boundary layer is specified, solely for the purpose of calculating the boundary-layer exchange coefficients. However, the velocity component equations are not linked in any other way as the Coriolis terms have been eliminated.

The model dimensions and initial parameters used are shown in Table 1. An idealized terrain profile was adopted of a half-bell-shaped hill with a lee side halfwidth of 1·6 km, and an upwind plateau 260 m above the coastal plain. This shape approximates the average profile of the escarpment (Fig. 1), constructed from 25 transects at 1 km intervals centred around the area flown (Pitts and Lyons 1989). The horizontal resolution was chosen to adequately resolve the halfwidth of the escarpment by equating it to three grid

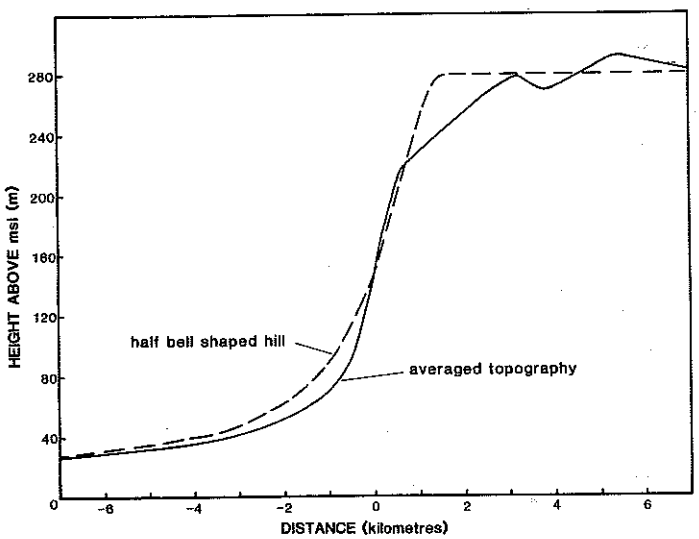


Figure 1. Average cross-section of escarpment and equivalent half-bell-shaped hill.

lengths (i.e. $3dx = a = 1{\cdot}6$ km), whereas the total number of horizontal grid points (100) was chosen to remove the lateral boundaries as far from the centre as possible (16·67 halfwidths), as well as provide a large plateau. For smaller plateaux, the material surface at the eastern edge of the plateau appeared to diverge. Hence with lateral boundaries set this far away, the original zero gradient conditions were employed (McNider and Pielke 1981) and not the lateral boundary conditions used by Durran and Klemp (1983). In the vertical, a stretched grid was used to ensure sufficient resolution to resolve sharp inversions whilst still enabling the model to reach an adequate height.

Given the arbitrary manner in which the Long filter coefficient is chosen and the possibilities of reflections from the absorbing layer and lateral boundaries, the model was validated by comparing it to results obtained by Klemp and Durran (1983). Their analysis addressed a hydrostatic, two-dimensional Boussinesq flow past a bell-shaped mountain and neglected the Coriolis force. Thus in our model the turbulence scheme was switched off and a freeslip bottom boundary layer employed. Consequently, for these validations, the north/south component of the velocity field was eliminated.

The model solution with a bell-shaped hill of halfwidth 1·6 km, height 300 m, wind speed 12 m s$^{-1}$ and $N = 0{\cdot}02\,\mathrm{s}^{-1}$, giving $Nh/U = 0{\cdot}5$, is plotted against nondimensional height ($Nz/U$) in Fig. 2(a) for the nondimensional time of $Ut/a = 54$. At this time the simulation should be approximating equilibrium flow (Klemp and Durran 1983) and compares favourably with Fig. 2(b) reproduced from Klemp and Durran (1983). Given that our model is incompressible but not Boussinesq, the solutions are similar although our solution is more damped, especially at higher levels, resulting from the action of the Long filter smoothing the fields and the proximity of the absorbing layer which commences at 5·6 km (i.e. $Nz/U = 9{\cdot}3$).

Results are plotted for the escarpment profile in Fig. 3. These show the higher nonlinearity and more pronounced steepening of the wave occurring at 0·5 the vertical wavelength, in agreement with Lilly and Klemp (1979).

## 3. Simulated days

Two days, 13 December 1986 and 3 February 1987, from the observations of Pitts and Lyons (1989) produced easily identifiable hydrostatically dominated flows and these were chosen for simulation. Upwind undisturbed temperature profiles were obtained from the eastern-most aircraft descent (Pitts and Lyons 1989) except for the 1620–2220 m layer of 3 February where there was evidence from the modelling that this layer's stability was influenced by blocking. Hence a higher stability was assumed. The wind profile was determined from the surface gradient wind speed with a constant wind shear used from the top of the boundary layer to the critical level. The boundary layer was assumed constant at 630 m above the surface. All of the data used to initialize the model are listed in Table 2.

These simulations were run until the solutions achieved quasi-equilibrium, generally corresponding to two hours, or a nondimensional time of approximately 50 (Durran and Klemp 1983). The resulting flows are plotted in Fig. 4 and illustrate general agreement with the observations of Pitts and Lyons (1989) reproduced in Fig. 5. Figure 4(a), based on data for 13 December, shows a broad 8 km trough and evidence of a wave in the 'near-neutral' layer at 1500–2300 m, whilst at approximately 2700 m there is little evidence of any activity. This is in agreement with the observations, except that they do not show any waves above 1500 m. The absence of an observed wave in the near-neutral layer is not conclusive as the small temperature differences involved make its resolution extremely difficult.

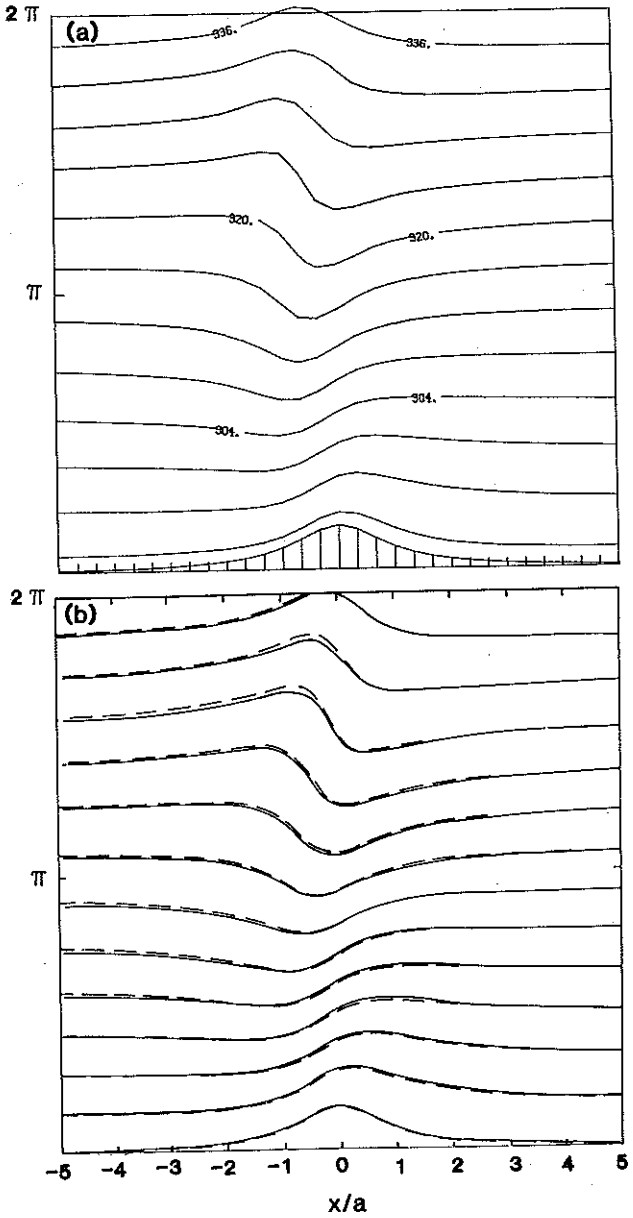


Figure 2. Predicted isentropic surfaces for a bell-shaped hill.
(a) Present model (for parameter values see text).
(b) Hydrostatic Boussinesq flow of Klemp and Durran (1983, nonlinear solution) with $Nh/U = 0{\cdot}5$ (solid lines); and nonlinear solution to Long's equation (McNider and Pielke 1984) (dashed lines).

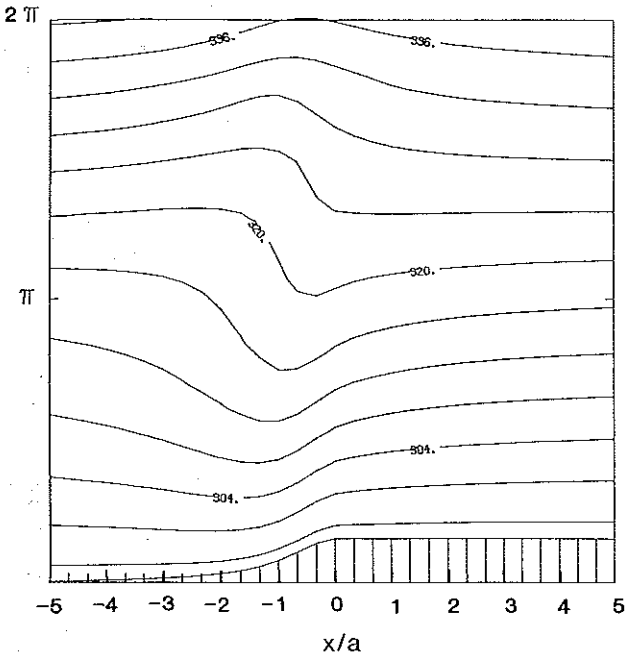


Figure 3. Predicted isentropic surfaces for an escarpment profile.

TABLE 2. INITIAL PROFILES FOR MODEL RUNS, BASED ON OBSERVATIONS OF PITTS AND LYONS (1989)

Surface potential temperature 288·5 K

Surface pressure 1016·0 hPa

Initial profiles

| 13 December 1986 | | | 3 February 1987 | | |
|---|---|---|---|---|---|
| Layer (m) | $N$ ($s^{-1}$) | $Nh/U$ | Layer (m) | $N$ ($s^{-1}$) | $Nh/U$ |
| 0– 760 | 0·005 | 0·078 | 0– 710 | 0·005 | 0·089 |
| 760– 890 | 0·050 | 0·892 | 710– 890 | 0·042 | 0·862 |
| 890–1520 | 0·0164 | 0·367 | 890–1620 | 0·018 | 0·619 |
| 1520–3300 | 0·0068 | ∞ | 1620–2220 | 0·015 | ∞ |
| 3300–7400 | 0·009 | | 2200–7400 | 0·010 | |

Gradient wind

17·7 m $s^{-1}$ 069° (13 December 1986); 15·6 m $s^{-1}$ 069° (3 February 1987)

Wind shear $-u$ component

| 13 December 1986 | | 3 February 1987 | |
|---|---|---|---|
| Layer (m) | Shear ($s^{-1}$) | Layer (m) | Shear ($s^{-1}$) |
| 0– 630 | none* | 0– 630 | none* |
| 630–2800 | 0·01 | 630–2000 | 0·0112 |
| 2800– | 0·00 | 2000– | 0·00 |
| Critical level | 2282 m | | 1930 m |

$-v$ component (constant above boundary layer)

6·34 m $s^{-1}$ (13 December 1986); 5·59 m $s^{-1}$ (3 February 1987)

* No wind shear enforced but boundary layer allowed to come to balance

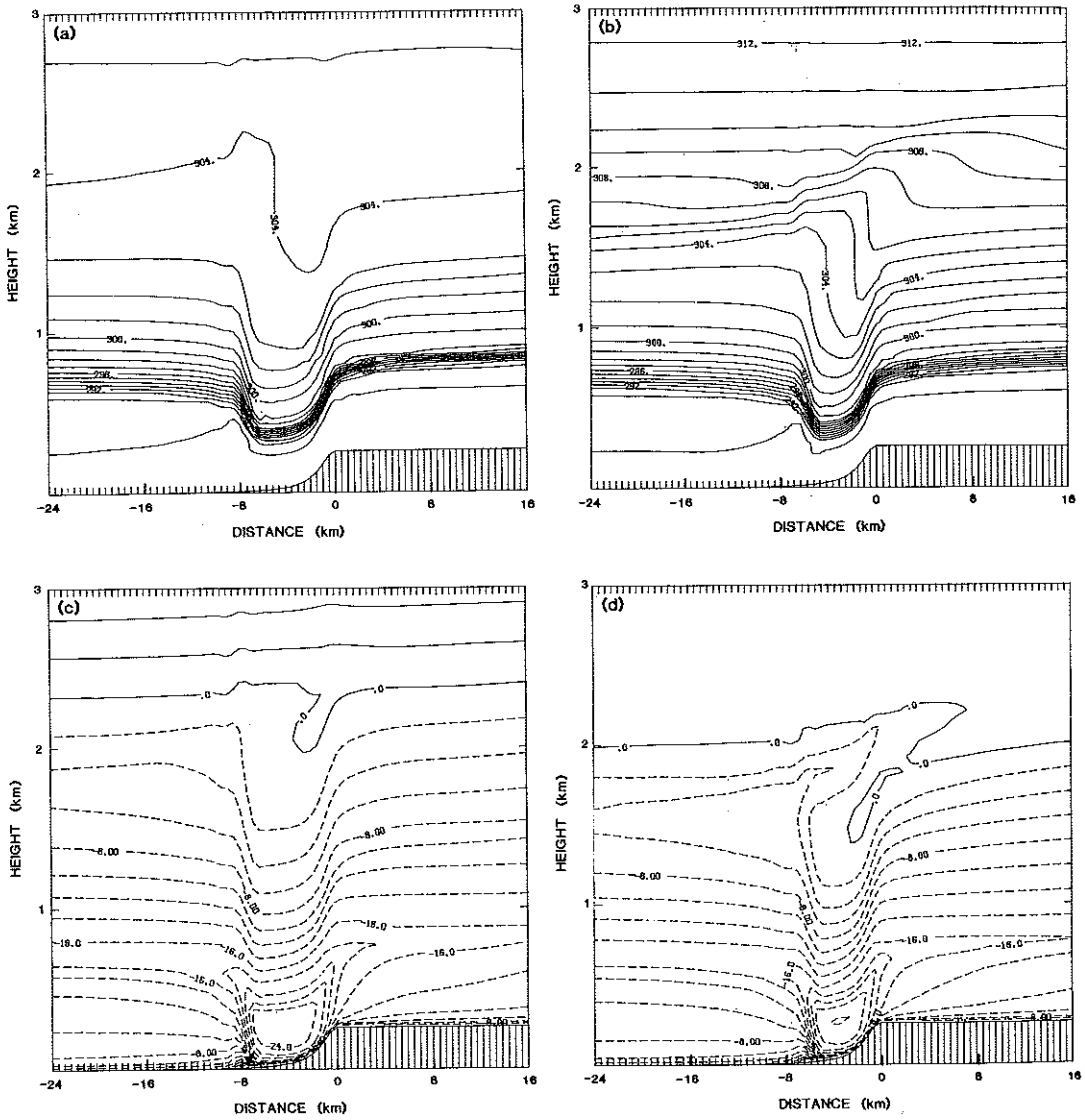


Figure 4. Model simulations of isentropic surfaces and $u$ component of the flow for 13 December (a, c) and 3 February (b, d).

Figure 4(b), for 3 February, clearly shows a vertically propagating internal gravity wave with a trough 6 km wide. This interacts with the surrounding air to produce a stable layer to the east of the escarpment above 2000 m and an inversion to the west of the escarpment at 1600–1800 m, in general agreement with the observations. The height of maximum wave steepening appears between 1400 and 1700 m, which is also in accord with the observations. However, the model isentropes, unlike the observations, indicate that the wave is overturning. This overturning is further seen in Fig. 4(d), where the wind turns westerly at approximately 1400 m. Such a discrepancy with the observations would not appear to be major given that the observed potential temperature fields were

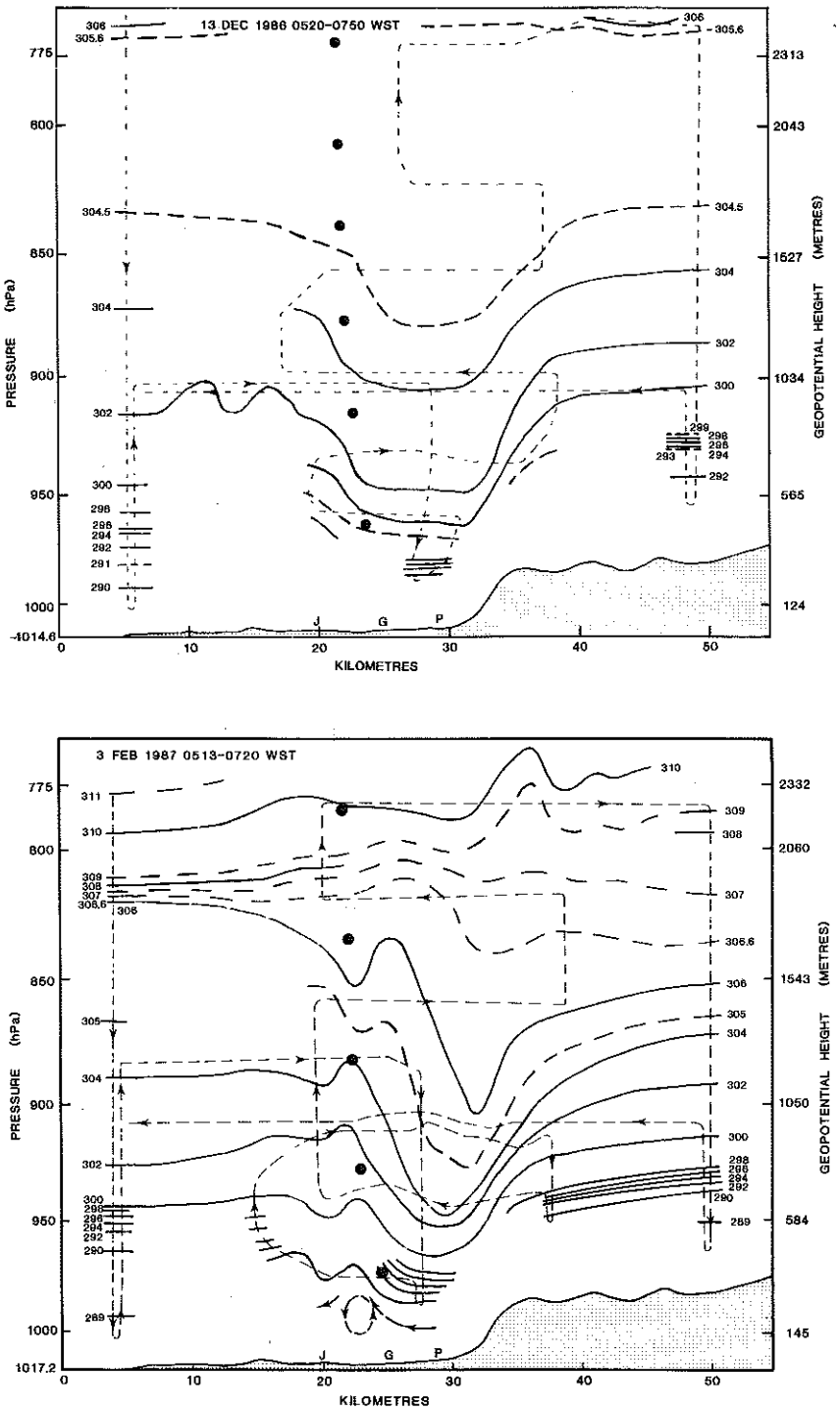


Figure 5. Observed isentropic surfaces for 13 December and 3 February (after Pitts and Lyons 1989).

interpolated from a succession of transects (Pitts and Lyons 1989). Nevertheless, it highlights a difficulty in the direct interpretation of the observations. The existence or otherwise of the overturning wave lends support to either hydraulic theory, as assumed by Pitts and Lyons (1989), in which a hydraulic jump develops from the overturning wave, or alternatively, Clark and Peltier's (1984) resonant amplification of the wave through reflection from the critical level.

The wind profiles for these two days both show the enhanced wind velocity to the lee of the escarpment with velocities of the order 1·5 times greater than the gradient wind speed. The magnitude of the maximum wind speed is very similar to that recorded by the Perth radiosonde, with a maximum of 21 m s$^{-1}$ on 13 December in the lowest 400 m agreeing well with the model results. Radar observations of the radiosonde on 3 February show an average wind speed of 24 m s$^{-1}$ in the 400–750 m layer (Pitts and Lyons 1988) which is not reproduced by the model, but may result from nonhydrostatic effects. For both these days, the model predicts the existence of a surface westerly flow to the lee of the updraught region (Figs. 4(c), (d)). This is in agreement with the rotor zone observed on 3 February (Pitts and Lyons 1988), whilst there was no evidence for this on 13 December. Just below the critical level, the results for 3 February show a stagnant layer much like those modelled by Clark and Peltier (1984), whilst for 13 December this feature is almost absent.

The simulations for both days appear to develop a shooting flow characteristic of hydraulic flow. February 3 may not be as obvious as 13 December because of the clear presence of a vertically propagating wave, but the shooting flow/trough still extends 7 km across the plain. Both days also appear to have wave overturning occurring and it is possible that the flows developed through the wave overturning because of the high nonlinearity of the flow and not because of reflection from some level. For overturning to occur in uniform conditions and constant density requires $Nh/U = 0{\cdot}85$ (Miles and Huppert 1969). However, for highly asymmetric topography, this value is reduced as a function of terrain shape (Lilly and Klemp 1979). Unfortunately, given the variable wind profile observed here, it is not possible to evaluate a characteristic $Nh/U$ for the flow, but the observations (Table 2; Pitts and Lyons 1989) suggest that 3 February clearly is nonlinear enough, whilst 13 December, with slightly lower values of $Nh/U$, would appear on average to be so.

## 4. Sensitivity analysis

These results were achieved using a boundary layer with a constant roughness length, $z_0$, of 50 cm. Across the region, land use ranges from an eucalyptus forest on top of the escarpment to urban areas and open land on the coastal plain. Consequently estimates of $z_0$ vary from 1 to 2 m on top of the escarpment to 7 cm (Kamst and Lyons 1982) on the coastal plain. The value of 50 cm was chosen as a representative average based on land use.

Smith (1979) notes that when the ratio of the height of the boundary layer to the mountain halfwidth becomes non-negligible then the boundary layer can no longer be neglected. Mahrer and Pielke (1978) also observed that the inclusion of a boundary layer significantly altered the solution, for a 1 km mountain with a halfwidth of 20 km, both near the ground and higher up. Nevertheless, most workers have employed a freeslip lower boundary condition in modelling much wider topography and have found the results adequate without resorting to this extra complication.

Enforcing a freeslip lower boundary condition for 3 February results in the solution shown in Fig. 6(a). This illustrates a very broad trough with its width increasing with

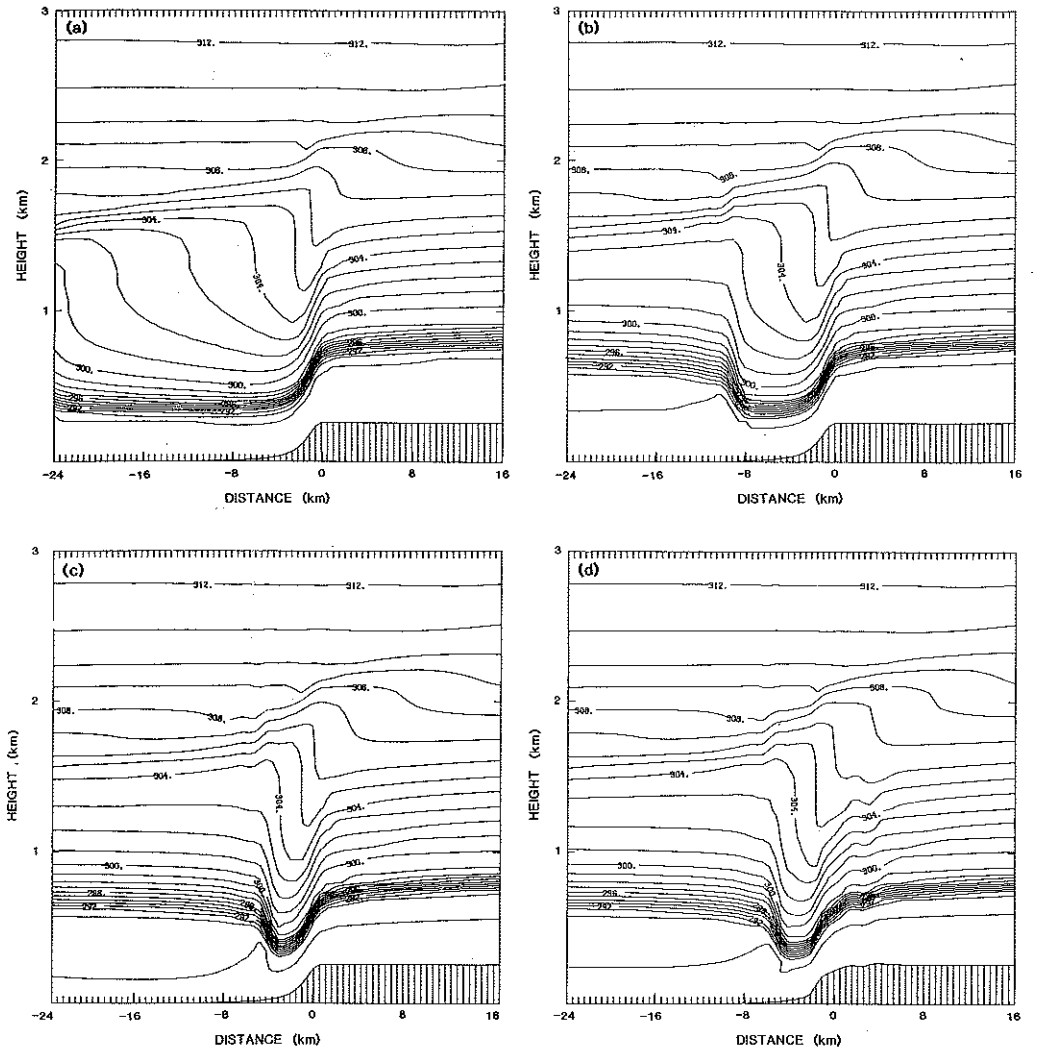


Figure 6. Predicted isentropic surfaces for 3 February assuming: (a) freeslip boundary conditions; (b) $z_o$ of 10 cm; (c) $z_o$ of 100 cm; and (d) average terrain profile rather than bell-shaped escarpment.

time. Clearly the inclusion of a boundary layer in the model is essential to reproduce the observed flow. The model was also run for $z_o$s of 10 and 100 cm and these results are shown in Figs. 6(b), (c). As the roughness length increases, the wave trough decreases in horizontal extent and the region of accelerated flow at the surface is decreased. This further highlights the sensitivity of the solutions to the boundary layer. The use of a constant $z_o$ for the whole domain gives reasonable results and simplifies the analysis but does not account for the variability of $z_o$ across the plain and the obvious sensitivity of the flow to such variations.

Instead of the idealized bell shape, the average escarpment profile shown in Fig. 1 was also used with a roughness length of 50 cm. These results (Fig. 6(d)) illustrate a solution similar to that obtained with the bell-shaped escarpment and a $z_o$ of 100 cm, although with a slightly wider trough. Of course, the use of such topography introduces a spectrum of wave numbers although the average profile has been filtered to remove all

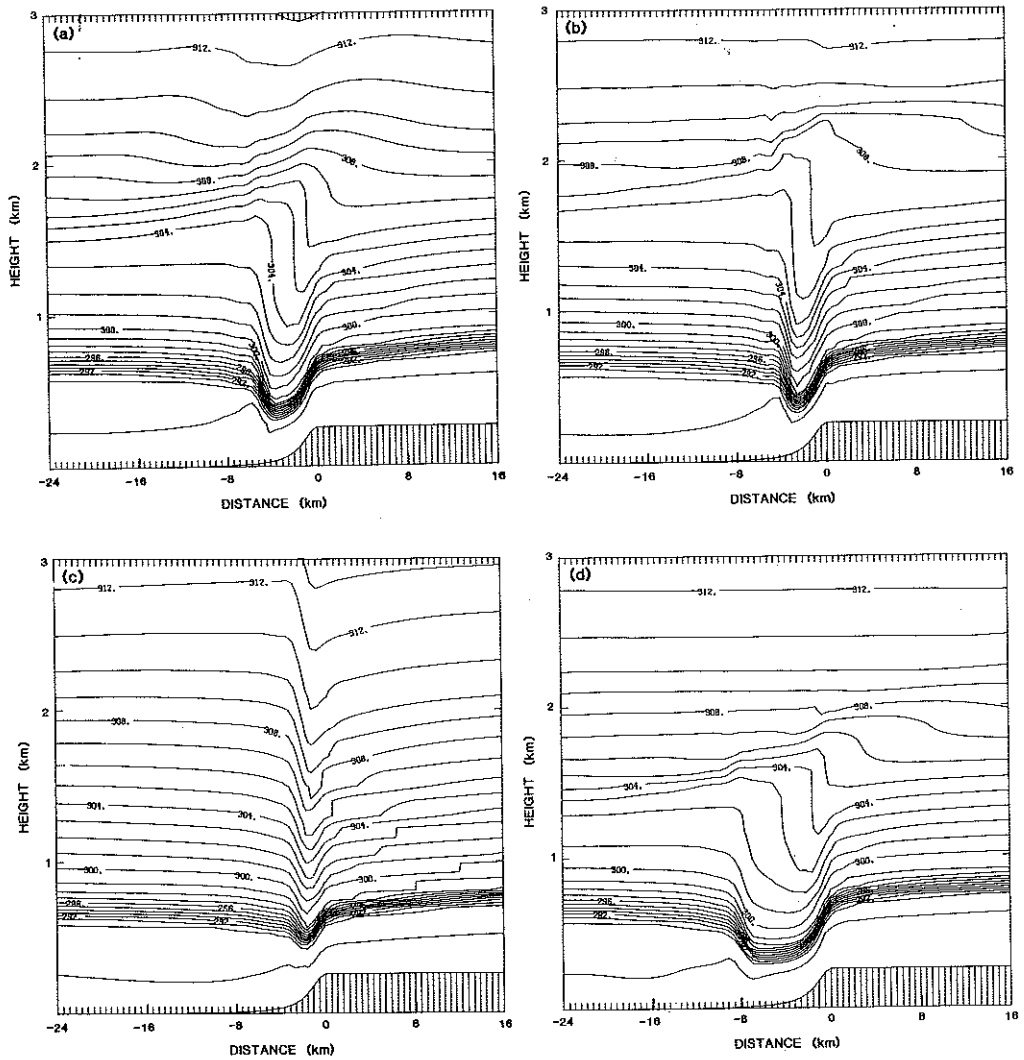


Figure 7. Predicted isentropic surfaces for 3 February assuming: (a) no critical level; (b) two-sheared wind profile; (c) constant wind speed profile; and (d) lower critical level.

short wavelengths that do not satisfy the hydrostatic approximation. Nevertheless, the mountain wavenumber is not as easily defined as with the simpler bell shape.

The observations of Pitts and Lyons (1989) are characterized by an inherent critical level and the influence of this was investigated by eliminating the wind shear above 1600 m for 3 February. The resulting simulation is shown in Fig. 7(a), where it is seen that this produces a similar flow to the original with a slightly narrower trough and propagation of wave energy further aloft. Thus the critical level is not essential in the development of the overturning wave and the associated shooting flow.

Maintaining the critical level at the same height but varying the wind profile by reducing the shear from the top of the boundary layer to 1500 m to $0{\cdot}006\,s^{-1}$ and from 1500 m to 2000 m to $0{\cdot}021\,s^{-1}$ results in the flow depicted in Fig. 7(b). Over the simulation time of two hours, the upper wind shear appeared to have broadened slightly by mixing

into the layer above. This slower decrease in wind speed over the majority of the flow to the critical level produces a much narrower wave.

Replacing the wind shear altogether by a constant wind speed of $15{\cdot}6\,\mathrm{m\,s^{-1}}$, 069°, results in the flow shown in Fig. 7(c). In this instance the wave does not overturn and wave energy is propagated vertically past 3 km. Also the vertical wavelength of the produced wave is much longer and the resultant maximum wind speeds occur further up the slope.

Figure 7(d) shows a simulation with a lower critical level at 1700 m and consequently a more highly sheared wind profile (i.e. $0{\cdot}014\,\mathrm{s^{-1}}$). As a wind shear of $0{\cdot}0112\,\mathrm{s^{-1}}$ produced overturning whether or not a critical level was present, this simulation with a higher $N/U$ and hence higher nonlinearity, would also be expected to overturn below the critical level. Figure 7(d) clearly illustrates, as expected, a more pronounced trough and the corresponding shooting flow associated with this higher wind shear.

Thus for 3 February, the simulations are not sensitive to the height of the critical level as the profile enables the wave to overturn below this level. This is similar to the simulations of the 15 April Bora flow by Klemp and Durran (1987) in which they proposed that the hydraulic flow developed through wave overturning in the highly nonlinear first layer. Bacmeister and Pierrehumbert (1988) also noted that when wave breaking occurs well below the critical level, the evolution of the high drag state is unlikely to be influenced by critical layer dynamics. The key requirement is wave breaking (Pierrehumbert and Wyman 1985), not the presence of an inherent critical level.

Our solutions are very sensitive to the wind profile, with a reduction in shear or a constant wind profile leading to a narrower wave which for the constant wind speed case does not overturn, and hence does not lead to a shooting flow. For higher wind shears the wave overturns, with the resultant shooting flow and the hydraulic jump further to the lee. This sensitivity appears to result from the influence of the wind speed on the nonlinearity of the flow and the resultant wavelength. For a rapidly decreasing wind speed, $N/U$ can remain large leading to a shorter wavelength and overturning. With a slower decrease in wind speed, the wavelength is larger and overturning may not occur. Thus, the wind profile would appear to be important in providing the necessary environment for wave breaking, and must be specified correctly. This also highlights the lack of an upwind profile as a major deficiency in the preliminary observations of Pitts and Lyons (1989).

The sensitivity of the flows to stability was investigated using the observations for 13 December. Initially the near-neutral layer between 1520 and 3300 m had its $N$ set equal to the $N$ of the layer below, that is $0{\cdot}0164\,\mathrm{s^{-1}}$. Such a modification produces no qualitative change in the temperature profile below 800 m and only a slight increase in the velocity (Fig. 8(a)). Above 800 m, however, the profile is now very similar to that observed and modelled for 3 February. Hence the 'near-neutral' layer does not appear to influence the production of the hydraulic flow near the surface. In both cases the wave overturns, with the more stable layer merely acting to transport more wave energy vertically, leading to larger perturbations in the velocity field aloft compared with the original simulation for 13 December.

Figure 8(b) shows a simulation wherein the inversion width has been halved, whilst the inversion strength was kept approximately the same. This solution illustrates little change from the original results, suggesting that the sharpness of the inversion is not a significant factor in determining the flow.

Figure 8(c) shows the resulting flow where the inversion has been eliminated by setting $N$ equal to $0{\cdot}0164\,\mathrm{s^{-1}}$ in the layer between 760 and 1520 m. In this case a broader trough develops, whilst there is a much weaker amplification of the velocities near the

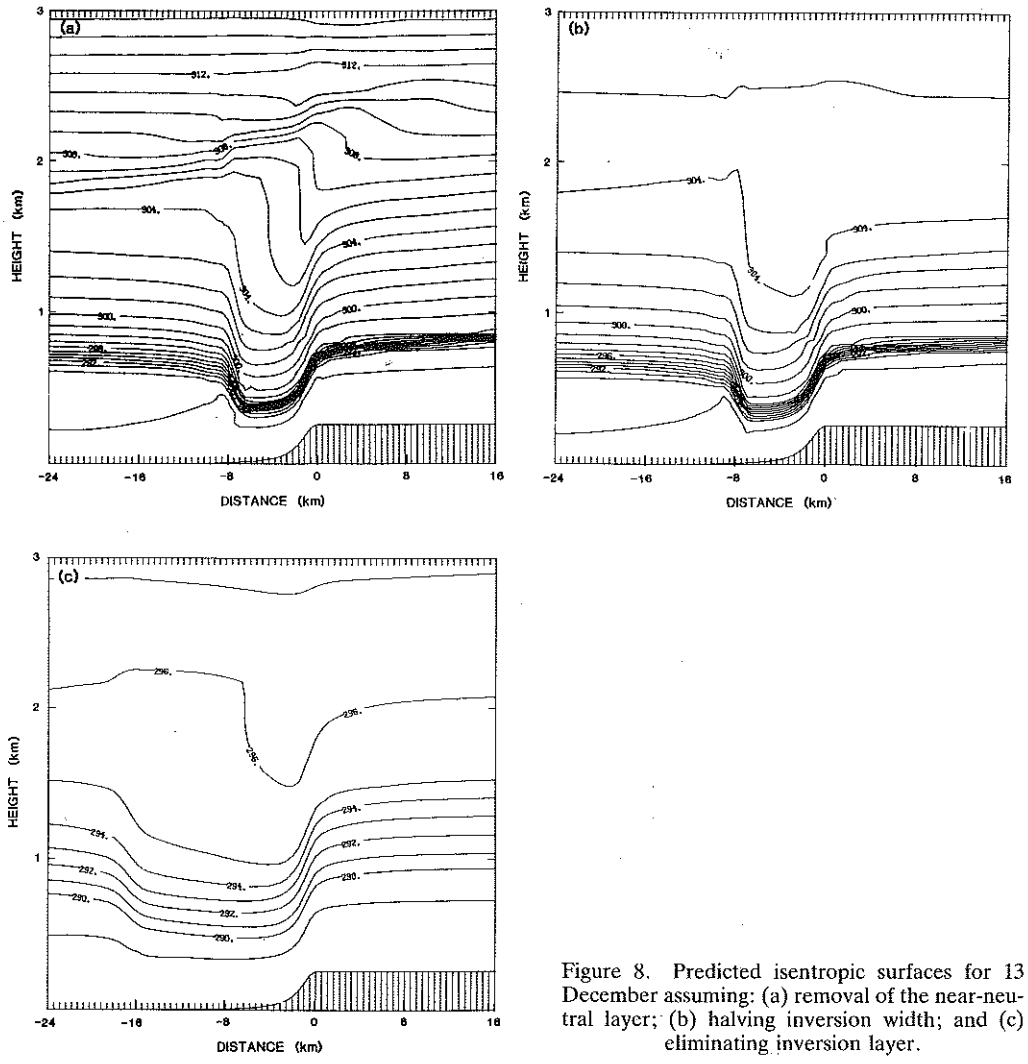


Figure 8. Predicted isentropic surfaces for 13 December assuming: (a) removal of the near-neutral layer; (b) halving inversion width; and (c) eliminating inversion layer.

ground. However, this flow cannot be considered hydrostatically dominated as $Na/U$ has now reduced to 2·19. Pitts and Lyons (1989) suggested that $Na/U \sim 4{\cdot}8$ represents a transition between hydrostatic and nonhydrostatic flows for this escarpment, which compares favourably with Klemp and Lilly's (1980) requirement of $Na/U > 10$ for propagating waves dominated by hydrostatic effects. Thus the modelled shooting flow is the result of the flow being unable to oscillate nonhydrostatically and is not valid.

The inversion observed on 3 February was also lowered by 120 m and raised by 120 m. The resulting flows showed little variation, with only a slight broadening and narrowing of the trough for the two cases respectively.

## 5. Conclusions

A modified hydrostatic mesoscale model, based on that described by McNider and Pielke (1981), has been compared against the validated model of Durran and Klemp (1983). Our solutions are similar although as a result of the explicit filtering employed,

appear slightly more damped. Nevertheless, this model is able to simulate two days of hydrostatically dominated flow (Pitts and Lyons 1989) over the highly asymmetric topography of the Darling Scarp. In both cases, the model predicts the production of a shooting flow and the acceleration of winds in the lee. As well, it indicates the development of a strong vertically propagating wave on 3 February and the correct deformation of the isentropes aloft with a much weaker wave and weaker deformation for 13 December.

The simulations also illustrate the similarity between the two flows, in that the shooting flow is minimally affected by the stability of the layer above 1500 m or by the presence of a vertically propagating wave at that level. Hence the stability profile on 13 December would appear to be more conducive to a larger shooting flow than that for 3 February. Thus, in accord with Klemp and Durran (1987), hydraulic flow developed through wave overturning in a highly nonlinear state. Wave breaking is the crucial requirement in maintaining the dynamics of the high drag state (Bacmeister and Pierrehumbert 1988).

The presence of a critical layer made minimal difference to both flows, although the development of the overturning wave was critically dependent on the wind profile. For the case of a slow decrease in the easterly wind speed with height, $N/U$ at the greater heights does not remain high, resulting in a longer wavelength and lower nonlinearity. This leads to a non-overturning, narrow wave with high wind speeds restricted to near the top of the escarpment. With a higher wind shear the flows developed a wider trough.

Simulations with a freeslip boundary condition and various roughness lengths showed the high sensitivity of the flow to the existence of a boundary layer. This sensitivity agrees with Smith (1979) and further confirms that for larger values of the ratio of boundary layer depth to mountain halfwidth, as found here, the solutions are sensitive to the boundary layer. Such high sensitivity, along with the previous simulations of Mahrer and Pielke (1978), point to the need to do further sensitivity tests for other mountains and flows.

Simulations with different temperature profiles showed very little sensitivity to the height (varied over 240 m for 3 February) or sharpness of the inversion (for 13 December).

## Acknowledgements

This study has been supported by the Australian Research Grants Scheme and Murdoch University's Special Research Grant. Throughout it, one of the authors (ROP) was in receipt of a Commonwealth Postgraduate Research Award. The figures were drafted by Mr Allan Rossow and Mr Mike Roeger. All of this assistance is gratefully acknowledged.

## References

Bacmeister, J. T. and Pierrehumbert, R. T. 1988 On high-drag states of nonlinear stratified flow over an obstacle. *J. Atmos. Sci.*, **45**, 63–80

Blackadar, A. K. 1979 High resolution models in the planetary boundary layer. Pp. 50–85 in *Advances in environmental and scientific engineering*, Vol. 1. Gordon and Breach

Clark, T. L. and Peltier, W. R. 1977 On the evolution and stability of finite-amplitude mountain waves. *J. Atmos. Sci.*, **34**, 1715–1730

1984 Critical level reflection and the resonant growth of nonlinear mountain waves. *ibid.*, **41**, 3122–3134

Durran, D. R. 1986 Another look at downslope windstorms. Part 1: The development of analogs to supercritical flow in an infinitely deep, continuously stratified fluid. *ibid.*, **43**, 2527–2543

| | | |
|---|---|---|
| Durran, D. R. and Klemp, J. B. | 1983 | A compressible model for the simulation of moist mountain waves. *Mon. Weather Rev.*, **111,** 2341–2361 |
| | 1987 | Another look at downslope winds. Part II: Nonlinear amplification beneath wave-overturning layers. *J. Atmos. Sci.*, **44,** 3402–3412 |
| Hoinka, K. P. | 1985 | A comparison of numerical simulations of hydrostatic flow over mountains with observations. *Mon. Weather Rev.*, **113,** 719–735 |
| Kamst, F. H. and Lyons, T. J. | 1982 | The evaluation of diffusivities for a non-uniform site. *Atmos. Environ.*, **16,** 379–390 |
| Klemp, J. B. and Durran, D. R. | 1983 | An upper boundary condition permitting internal gravity wave radiation in numerical mesoscale models. *Mon. Weather Rev.*, **111,** 430–444 |
| | 1987 | Numerical modelling of Bora winds. *Meteorol. Atmos. Phys.*, **36,** 215–227 |
| Klemp, J. B. and Lilly, D. K. | 1975 | The dynamics of wave-induced downslope winds. *J. Atmos. Sci.*, **32,** 320–339 |
| | 1978 | Numerical simulation of hydrostatic mountain waves. *ibid.*, **35,** 78–107 |
| | 1980 | Mountain waves and momentum flux. Pp. 116–141 in *Orographic effects in planetary flows.* GARP Series No. 23. W.M.O. |
| Lilly, D. K. | 1978 | A severe downslope windstorm and aircraft turbulence event induced by a mountain wave. *J. Atmos. Sci.*, **35,** 59–77 |
| Lilly, D. K. and Klemp, J. B. | 1979 | The effects of terrain shape on nonlinear hydrostatic mountain waves. *J. Fluid Mech.*, **95,** 241–261 |
| Lilly, D. K. and Zipser, E.J. | 1972 | The front range windstorm of 11 January 1972: a meteorological narrative. *Weatherwise*, **25,** 56–63 |
| Long, R. R. | 1954 | Some aspects of the flow of stratified fluids. II. Experiments with a two-fluid system. *Tellus*, **6,** 97–115 |
| Mahrer, Y. and Pielke, R. A. | 1977 | A numerical study of the airflow over irregular terrain. *Contrib. Atmos. Phys.*, **50,** 98–113 |
| | 1978 | A test of an upstream interpolation technique for the advective terms in a numerical mesoscale model. *Mon. Weather Rev.*, **106,** 818–830 |
| McNider, R. T. and Pielke, R. A. | 1981 | Diurnal boundary layer development over sloping terrain. *J. Atmos. Sci.*, **38,** 2198–2212 |
| | 1984 | Numerical simulation of slope and mountain flows. *J. Climate Appl. Meteorol.*, **23,** 1441–1453 |
| Miles, J. W. and Huppert, H. E. | 1969 | Lee waves in a stratified flow. 4. Perturbation approximations. *J. Fluid Mech.*, **35,** 497–525 |
| Peltier, W. R. and Clark, T. L. | 1979 | The evolution and stability of finite-amplitude mountain waves. Part II. Surface wave drag and severe downslope windstorms. *J. Atmos. Sci.*, **36,** 1498–1529 |
| | 1983 | Nonlinear mountain waves in two and three spatial dimensions. *Q. J. R. Meteorol. Soc.*, **109,** 527–548 |
| Pielke, R. A. | 1974 | A three-dimensional numerical model of the sea breeze over south Florida. *Mon. Weather Rev.*, **102,** 115–139 |
| Pielke, R. A. and Mahrer, Y. | 1975 | A numerical study of the airflow over mountains using the two-dimensional version of the University of Virginia mesoscale model. *J. Atmos. Sci.*, **32,** 2144–2155 |
| | 1978 | Verification analysis of the University of Virginia three-dimensional mesoscale model prediction over South Florida for 1 July 1973. *Mon. Weather Rev.*, **106,** 1568–1589 |
| Pierrehumbert, R. T. and Wyman, B. | 1985 | Upstream effects of mesoscale mountains. *J. Atmos. Sci.*, **42,** 977–1003 |
| Pitts, R. O. and Lyons, T. J. | 1988 | The influence of topography on Perth radiosonde observations. *Aust. Meteorol. Mag.*, **36,** 17–23 |
| | 1989 | Airflow over a two-dimensional escarpment. I: Observations. *Q. J. R. Meteorol. Soc.*, **115,** 965–981 |
| Smith, R. B. | 1979 | The influence of mountains on the atmosphere. *Adv. Geophys.*, **21,** 87–230 |
| | 1985 | On severe downslope winds. *J. Atmos. Sci.*, **42,** 2598–2603 |
| Smith, R. B. and Sun, J. | 1987 | Generalized hydraulic solution pertaining to severe downslope winds. *ibid.*, **44,** 2934–2939 |